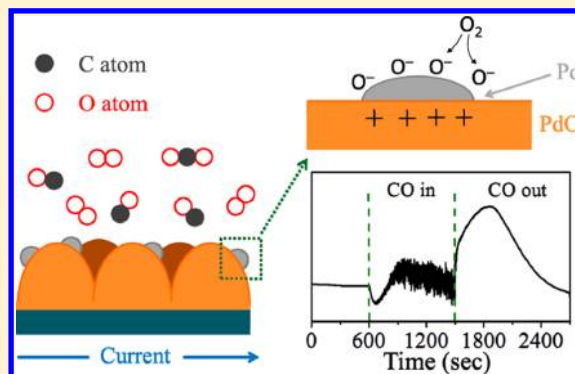


PdO Nanoflake Thin Films for CO Gas Sensing at Low Temperatures

Yu-Ju Chiang and Fu-Ming Pan*

Department of Materials Science and Engineering, National Chiao Tung University, 1001 Ta Hsueh Road, Hsinchu, Taiwan 30010, R.O.C.

ABSTRACT: We prepared PdO nanoflake thin films by reactive sputter deposition and studied their gas-sensing response to CO at temperatures below 250 °C. The PdO thin film, which has a large open surface area allowing for rapid and extensive CO adsorption, exhibits a complicated CO sensing behavior. At temperatures below 150 °C, the electrical conductance of the thin film drops upon the exposure of the CO/dry air gas mixture. The CO sensing mechanism in this temperature range is described by the oxygen ionosorption model. At 150 °C, oscillatory response occurs when the CO concentration is larger than 2000 ppm. The oscillatory response is due to the reactivity switching between the PdO reduction and reoxidation reactions. In addition, the PdO thin film shows a rapid increase in the conductance before and after the oscillatory response regime. The conductance increase is ascribed to the positive charge accumulation at the interface between the PdO thin film and metal Pd nanoislands, which are formed during the PdO reduction. At temperatures higher than 150 °C, the conductance drops when the PdO thin film is exposed to CO. Besides the ionosorption model, the oxygen vacancy model is used to account for the CO sensing response of the thin film in the high-temperature range. On the basis of the inverse change in the CO sensing sensitivity at 150 °C, a CO sensor of high selectivity, which integrates two PdO sensing elements operating independently at 150 °C and a lower temperature, is proposed.



1. INTRODUCTION

Carbon monoxide (CO) is a colorless, odorless, tasteless, toxic gas. CO emission typically results from incomplete combustion of hydrocarbons and is one of the major gases released at the initial stage of fire incidents.¹ Because CO molecules have a higher affinity for human blood hemoglobin than oxygen molecules, unintentional inhalation of a trace amount of CO may lead to lethal accidents. Therefore, effective and reliable monitoring of trace CO gas is important to avoid such unfortunate accidents due to the CO poisoning. Many kinds of CO gas sensors have been developed for this purpose, including aqueous and nonaqueous electrolyte gas sensors,² optical gas sensors,^{3–5} and oxide semiconductor gas sensors.^{6–18} Among these sensors, oxide semiconductor sensors have been the most widely studied because of their higher sensitivity, faster response, better stability, and lower maintenance costs.¹⁹ Both n- and p-type oxide semiconductors have been explored for gas sensor applications. However, n-type oxide semiconductors, such as TiO₂,^{6,7} ZnO,^{8–11} and SnO₂,^{12–15} receive much more attention than p-type oxide semiconductors, such as CuO¹⁶ and Co₃O₄.^{17,18}

The gas-sensing behavior of oxide semiconductors is generally described by the oxygen ionosorption model and the oxygen vacancy model.^{20,21} The former model is based on the charge transfer between adsorbed oxygen molecules and oxide semiconductors, which results in the formation of anionic oxygen adspecies, such as superoxide (O₂⁻) and peroxide (O₂²⁻) ions. The charge transfer effect leads to the development

of a space charge region on the oxide surface and thus the change in the electrical conductivity of the semiconductors.^{22,23} When an oxide semiconductor is exposed to a reducing gas, such as CO and H₂, the depletion of oxygen adspecies due to interactions with the reducing gas can restore the conductivity of the oxide semiconductor. In the oxygen vacancy model, reducing gases directly interact with the oxide lattice at high temperatures, producing oxygen vacancies and thus increasing the free electron concentration in the oxide semiconductor.^{24,25} As far as low-temperature gas sensing is concerned, the ionosorption model is more appropriate for the description of the gas-sensing behavior of oxide semiconductors. Because p-type oxide semiconductors are apt to adsorb oxygen,^{26–28} they should be a sensitive sensor for the detection of reducing gases at low temperatures.

In the study, we prepared PdO nanoflake thin films on a SiO₂/Si substrate and studied its gas-sensing response to CO at temperatures below 250 °C. PdO is a p-type oxide semiconductor with a band gap around 2.2 eV²⁹ and has stable chemical properties and high thermal stability. Molecular oxygen can form relatively strong binding states on PdO.³⁰ Hence, the gas-sensing behavior of PdO at low temperatures can be properly described by the ionosorption model. We believe that PdO must have a sensitive response to CO

Received: February 28, 2013

Revised: May 9, 2013

Published: July 8, 2013

adsorption because of its active role in the Pd oxidation reaction with reducing gases. Palladium has been widely used as the catalyst for low-temperature oxidation of CO and hydrocarbons. Although a conclusive reaction mechanism is still not available for the catalytic CO oxidation using Pd as the catalyst, many studies suggest that PdO is the active phase in the catalytic reaction.^{31,32} According to this study, the PdO thin film exhibits different sensing behaviors toward CO in different temperature ranges. Most interestingly, an oscillatory sensing response was observed to occur at 150 °C in the CO/dry air gas mixture; the oscillatory response is related to the occurrence of the alternating PdO reduction and reoxidation reactions.

2. EXPERIMENTAL SECTION

2.1. Preparation of PdO Nanoflake Thin Films. PdO nanoflake thin films were deposited on the SiO₂/Si substrate by reactive sputter deposition at room temperature. The palladium target with a purity of 99.99% was 2 in. in diameter. The PdO deposition was performed with a gas mixture of argon (20 sccm) and oxygen (20 sccm) at a working pressure of 9×10^{-3} Torr and the rf power of 50 W. The as-deposited thin film was annealed in an atmospheric furnace at 400 °C for 2 h. The surface morphology of the PdO nanoflake thin film was examined by scanning electron microscopy (SEM) (JEOL JSM-6500F), and the chemical composition was characterized by X-ray photoelectron spectroscopy (XPS) (thermo VG 350) with the Mg K α X-ray source. The XPS spectra presented in the study have been calibrated with the Pt 4f_{7/2} binding energy. The XPS spectrum curve fitting was performed using the Shirley background subtraction method and assuming a Gaussian and Lorentzian peak shape. The microstructure of the thin film was analyzed by transmission electron microscopy (TEM) (JEOL JEM-3000F) and an X-ray diffractometer (XRD) (Bruker AXS D8) using the Cu K α radiation.

2.2. CO Gas Sensing Measurement of PdO Nanoflake Thin Films. For gas-sensing experiments, the PdO thin film specimen was cut into a size of 2×1 cm². Both ends of the specimen were coated with conductive silver paste as the electrodes, leaving an open area of 1.5×1 cm² for the gas-sensing test. The specimen was then dried in an oven at 60 °C for 2 h to remove volatile impurities in the paste. The CO-gas-sensing experiment was conducted at the atmospheric pressure in a stainless steel chamber. Because PdO absorbs visible light, the test chamber was shielded from light to avoid the generation of photocurrent. The dry air was used as the reference gas and the CO source was a gas mixture of 1% CO and 99% dry air. The CO concentration for the sensing experiment was adjusted by varying the volume ratio of the dry air and the CO gas mixture using mass flow controllers. The CO gas mixture was conducted into a mixer to enhance the gas uniformity before it was introduced into the test chamber. During the gas-sensing test, the total flow rate of the CO gas mixture and the reference gas was maintained at 200 sccm. The change in the conductance of the PdO thin film upon the CO exposure was monitored by a Keithley 237 source-measure unit. The samples were biased at 1 V during the sensing test. A pristine PdO specimen was used for each separate sensing test so that the sensor specimens had similar surface properties for every test.

3. RESULTS AND DISCUSSION

The as-deposited PdO thin film has a morphology of interconnecting nanoflakes, and the thin film sustains its nanoflake feature after thermal annealing at temperatures up to 500 °C. Figure 1 shows SEM images of a PdO nanoflake thin

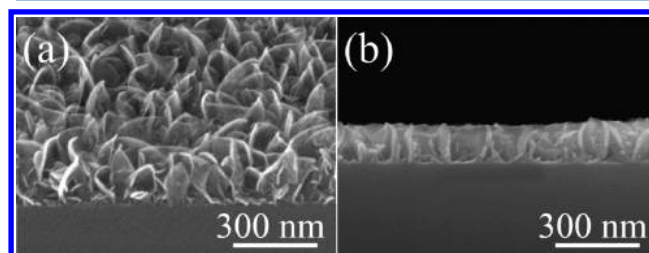


Figure 1. SEM images of the PdO nanoflake thin film thermally annealed at 400 °C for 2 h: (a) the tiled-view and (b) the cross-sectional images.

film thermally annealed at 400 °C. The nanoflakes have a height of approximately 140 nm and a length smaller than 150 nm. From the tilting SEM image, PdO nanoflakes on the thin film are partially transparent, indicating an extremely small thickness. A rough estimation from the SEM image gives a thickness of 15–20 nm for the nanoflakes. XPS spectra reveal that PdO is the only chemical state on the surface of the PdO thin film. X-ray diffraction analysis shows that the nanoflake thin film is well-crystalline after thermal annealing at 400 °C, as indicated by characteristic peaks of the PdO tetragonal lattice structure (not shown). Because of the ultrathin thickness of the nanoflake, the space charge region induced by O₂ adsorption can occupy most volume of the nanoflake, resulting in a very sensitive change in the electrical conductivity of the film. Moreover, the PdO nanoflake thin film has an open surface with a large area, and gas adsorption on the thin film should be extensive and rapid, thereby enhancing the gas-sensing performance. In the following discussion about gas-sensing experiments, a PdO thin film annealed at 400 °C was used as the test sample.

Figure 2 shows the gas-sensing response of the PdO thin film at 50 °C as a function of the measurement time for different CO concentrations. Each current–time profile was obtained by periodically exposing an as-prepared PdO sample to the CO/dry air gas mixture. From Figure 2, the PdO thin film shows little sensing response at 50 °C to the gas mixture with a CO concentration smaller than 250 ppm. However, when the CO concentration reaches 500 ppm and higher, the sensing current rapidly drops upon the introduction of the CO gas mixture. The current decrease suggests a reduction in the majority carrier concentration of the p-type PdO thin film. The PdO thin film had little change in the chemical state after the exposure of the CO/dry air mixture according to XPS analysis (not shown). In other XPS experiments to be discussed later, Pd maintained its oxidation state after the PdO thin film was annealed in a gas mixture of 1% CO and N₂ at 90 °C. We thus believe that the drop in the sensing current must result from interactions of CO adspecies with adsorbed oxygen, but not with the PdO surface lattice. It has been reported that molecularly chemisorbed O₂ on the PdO(101) surface plays an active role in the oxidation of adsorbed CO.³⁰ In a study on CO adsorption on the PdO(100) surface based on density functional calculations, Hirvi et al. suggested that adsorbed oxygen molecules may react with CO adspecies at relatively low

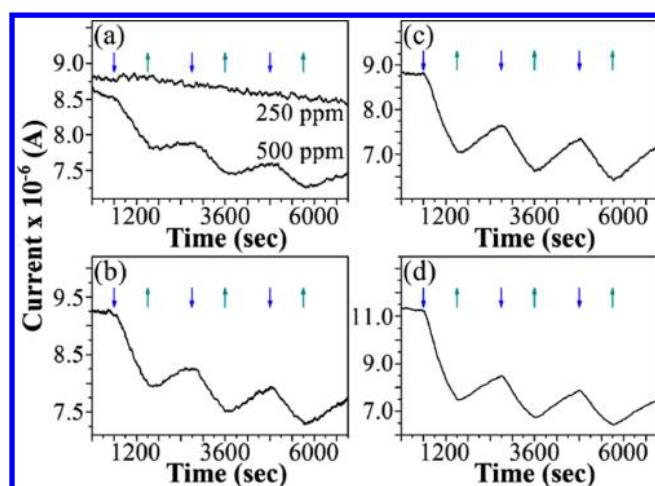


Figure 2. The CO sensing current of the PdO thin film as a function of the test time, which was exposed to the gas mixture of different CO concentrations at 50 °C: (a) 250 and 500 ppm, (b) 1000 ppm, (c) 2000 ppm, and (d) 4000 ppm. The downward and upward arrows indicate the times when the flow of the CO gas mixture is opened and closed, respectively.

temperatures, leading to the formation of stable carbonate species.³³ According to the oxygen ionsorption model, oxygen adsorption on an oxide semiconductor at temperatures below 150 °C results in charge transfer between adsorbed oxygen molecules and the semiconductor, forming O_2^- anionic adspecies and creating an electron-depleted zone in the surface layer of the semiconductor. The electron-depleted zone decreases the majority carrier concentration of n-type oxide semiconductors. In contrast, oxygen adsorption on p-type oxides creates an accumulation zone, thereby increasing the electrical conductance of the oxide. If the ionsorption model holds for the PdO thin film, the developed accumulation zone should occupy a large volume portion of the thin film because the PdO nanoflake is extremely thin. In consequence, the O_2^- adsorption should greatly increase the conductance of the PdO thin film. On the other hand, CO oxidation with O_2^- can decrease the coverage of the anionic adspecies on the PdO thin film, resulting in the diminution of the accumulation zone and thus an obvious drop in the sensing current. Moreover, CO is generally regarded as an electron donor on metal oxides.³⁴ Negative charge transfer from adsorbed CO molecules to the PdO thin film can reduce the hole concentration of the oxide, further decreasing the conductance.

The PdO thin film exhibits a stepwise drop in the conductance at each exposure cycle of the 500 ppm CO gas mixture according to Figure 2. The stepwise conductance drop implies that the coverage of CO-related adspecies on the PdO surface increases by each CO exposure cycle, resulting in the successive decrease in the conductance. When the 500 ppm CO gas flow is closed, the measured current increases at a very slow rate to a saturation level that is lower than the initial value of each corresponding CO exposure cycle. We shall thereafter refer to the measured current after the stop of the CO gas flow as the “recovery current”. In another experiment that monitored the recovery current for more than 1 h after the 500 ppm CO exposure of 15 min, the saturation current was about 92% of the initial value before the exposure. For a longer CO exposure, the saturation value becomes lower. The lower conductance than the initial value suggests that the original surface condition of the PdO sensor cannot be restored after

the CO exposure, and most of the adspecies, including CO and oxygen, are likely to retain their adsorption structure on the surface of the PdO thin film at 50 °C. However, weakly adsorbed CO molecules may eventually be desorbed from the PdO surface, leaving free sites for oxygen readsorption, which in turn increases the majority carrier concentration of the p-type oxide thin film. Thus, the observed slow increase in the recovery current can be ascribed to the desorption of weakly adsorbed CO molecules. CO exhibits different adsorption strength on various PdO planes. For example, CO has a very weak adsorption energy on the PdO(100) surface (−0.03 eV), while it is strongly bound on the PdO(101) surface with an adsorption energy of −1.46 eV.³³ Because of the irregular shape, the PdO nanoflake must have various orientations and defects on the surface, and hence, there should be many different CO adsorption states on the PdO thin film with different adsorption strengths. In the case of the low CO exposure, most CO adspecies should be strongly bound on PdO adsorption sites, but some may still be weakly adsorbed on the surface. When thermally annealing the 500 ppm CO-exposed PdO thin film in air at 100 °C for 15 min, we found that the conductance of the thin film was nearly restored to the initial value, implying that strongly bound CO adspecies can also be desorbed from the PdO thin film at high temperatures. This observation is consistent with the experimental result for CO gas sensing at 100 °C, which will be discussed later. On the basis of the successive reduction in the conductance at each exposure cycle, we believe that CO adsorption on the PdO thin film is more favorable than oxygen adsorption in the low-temperature regime. Without a faster adsorption kinetics, CO adsorption on the PdO thin film can hardly compete with O_2 adsorption because CO in the gas mixture has a much smaller concentration than oxygen.

For samples exposed to a gas mixture with the CO concentration larger than 500 ppm, the sensing behavior is similar to that with the 500 ppm CO gas. However, they have a larger and more rapid conductance drop when CO gas is introduced and show a higher increase rate of the recovery current. At higher CO concentrations, more PdO surface sites can be occupied by CO adspecies because of the concentration equilibrium established between the CO gas phase and the adsorption phase. As a consequence, the high CO exposure results in a rapid drop in the conductance of the thin film. When the CO gas is switched off, a significant amount of weakly adsorbed CO molecules leave from the oxide surface because of their small adsorption energy, leading to the observation of the large increase rate of the recovery current. However, the recovery current never returns to the initial current level; the saturation current at the first exposure cycle is 87% and 79% of the initial value for the 1000 and 2000 ppm CO exposures, respectively. The reduced conductance indicates that the majority of PdO surface sites are steadily occupied by CO adspecies at 50 °C after the CO gas flow is stopped.

Figure 3 shows the CO sensing response of the PdO thin film at different temperatures using the 2000 ppm CO gas mixture. In the temperature range between 25 and 100 °C, the PdO thin film has a steeper conductance drop at higher temperatures in response to the CO exposure. The current drop at 100 °C exhibits an exponential decay behavior, which is not obvious at lower temperatures. It is likely that a surface reaction similar to that occurring at 25 and 50 °C is kinetically favored at 100 °C; the reaction can quickly consume O_2^- adspecies and thus lead to the rapid drop in the conductance.

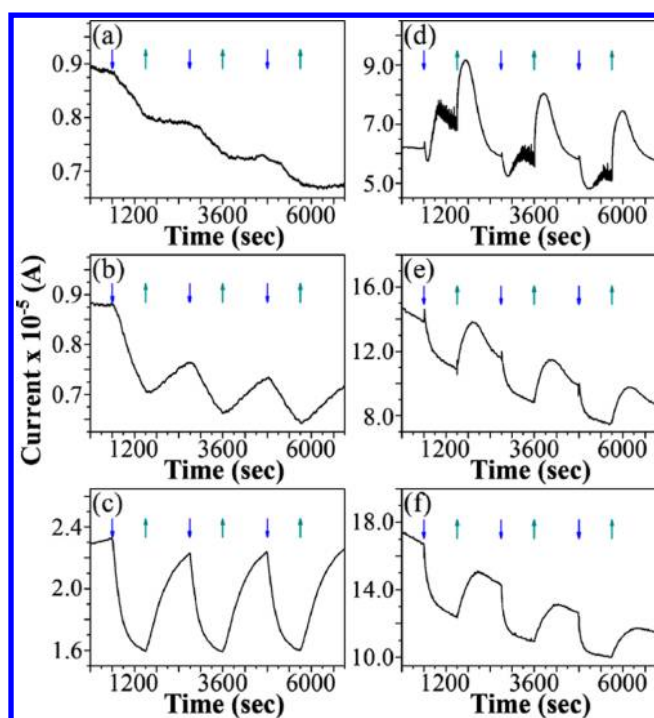


Figure 3. The CO sensing current of the PdO thin film exposed to the 2000 ppm CO gas mixture at different temperatures: (a) 25 °C, (b) 50 °C, (c) 100 °C, (d) 150 °C, (e) 200 °C, and (f) 250 °C. The downward and upward arrows indicate the times when the flow of the CO gas mixture is opened and closed, respectively.

The increase in the recovery current at 100 °C is much more rapid than at 25 and 50 °C, and the conductance almost returns to the initial level of the as-prepared PdO thin film, indicating that the chemical modification on the PdO surface by the CO exposure is insignificant. As discussed previously for the CO sensing at 50 °C, the conductance increase of the PdO thin film after the stop of the CO gas flow is due to the desorption of weakly adsorbed CO from the PdO surface. At higher temperatures, both weakly and strongly bound CO adspecies can be desorbed effectively from the PdO thin film, leaving a CO-free surface. Oxygen readsorption can then take place on the entire surface of the PdO thin film in the dry air, thus restoring the conductance of the thin film nearly to the initial level.

At temperatures around 150 °C, the PdO thin film exhibits an oscillatory sensing response to CO, but the response is perceptible only when the CO concentration is larger than 1500 ppm. Figure 4 shows the sensing response of the PdO thin film at 150 °C for different CO concentrations. Although the oscillatory response does not show a regular oscillation pattern, a rough estimation gives the average oscillation period of 13 s, as shown in Figure 4d, which shows an enlarged time zone in the second exposure cycle for the 4000 ppm CO gas mixture. Kinetic oscillation is well-known to occur in catalytic CO oxidation on Pt-group metals and is generally ascribed to the switching in the reactivity of CO oxidation due to the alternating oxidation and reduction of the metal.^{35–38} The oscillatory CO sensing response of the PdO thin film must also result from a similar mechanism, namely, alternating PdO reduction and Pd oxidation occur on the PdO nanoflakes during the exposure of the CO/dry air gas mixture. Under the oxygen-rich reaction condition, the metal Pd phase produced as a result of the PdO reduction is continually formed and

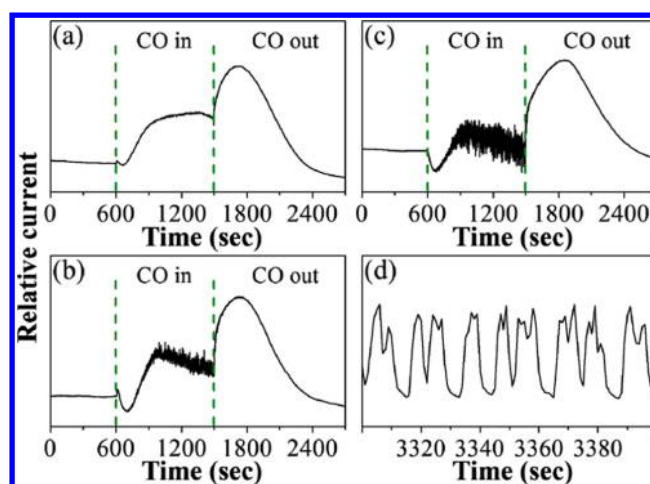


Figure 4. The relative CO sensing current of the PdO thin film at 150 °C for different CO concentrations of (a) 1000 ppm, (b) 2000 ppm, and (c) 4000 ppm and (d) an enlarged time zone for the 4000 ppm CO gas mixture. Each CO sensing test comprises three CO exposure cycles, but only the first cycle is shown. The enlarge time zone shown in part d is in the second exposure cycle for the 4000 ppm CO gas mixture.

consumed. Because the metal Pd phase can be quickly reoxidized in the dry air at 150 °C, ex situ XPS analysis cannot reveal the presence of the metal state after the CO-gas-sensing experiment. To investigate if metal Pd can be formed at 150 °C as a result of PdO reduction by CO, we performed temperature programmed desorption (TPD) for a CO-adsorbed PdO thin film in a vacuum system with the base pressure of 1×10^{-6} Torr. The PdO nanoflake thin film was exposed to a gas mixture of 1% CO and N₂ at 5×10^{-4} Torr at room temperature. The TPD spectrum in Figure 5 shows an asymmetric CO₂ desorption peak spanning a temperature range between 110 and 150 °C, suggesting that PdO reduction by CO is likely to occur at temperatures higher than 110 °C. In addition, both XPS and TEM analyses show the formation of metal Pd on the PdO thin film that was thermally annealed at 110 °C in a gas mixture of 1% CO and N₂ at 10 Torr. Figure 6a

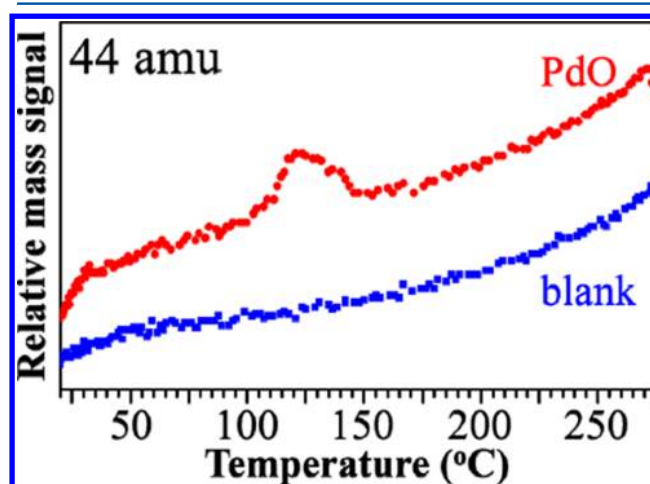


Figure 5. The TPD spectrum of CO₂ produced from the PdO thin film which was exposed to the gas mixture of 1% CO and N₂ at 5×10^{-4} Torr at room temperature. TPD spectrum of a PdO thin film without the CO exposure is also shown in the figure for comparison. The sample was heated at a linear rate of 2 °C/s.

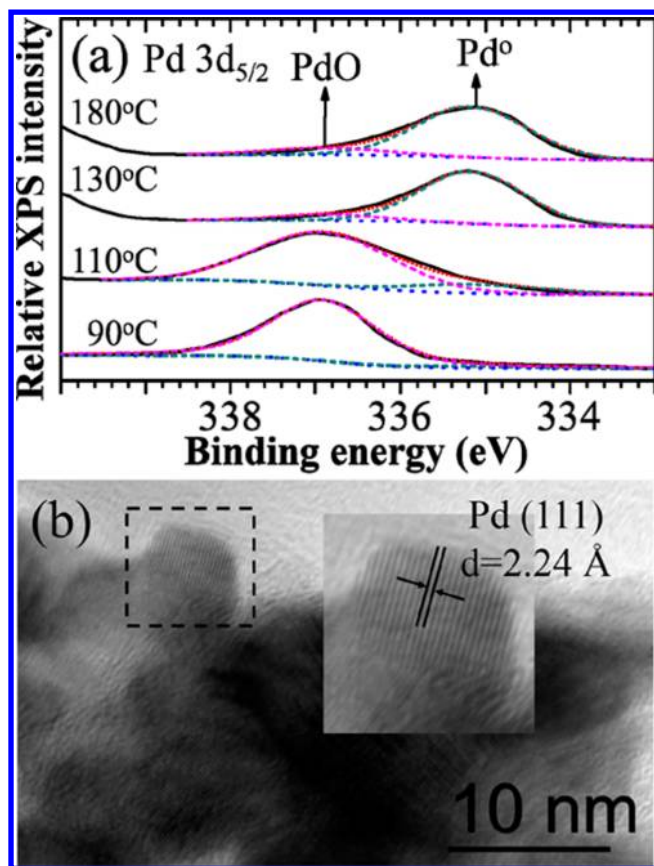


Figure 6. Pd $3d_{5/2}$ XPS spectra (a) and the HRTEM image (b) of the PdO nanoflake thin film thermally annealed in a gas mixture of 1% CO and N₂ at 10 Torr. The annealing temperature of the XPS samples is labeled above each corresponding spectrum. The TEM specimen was annealed at 110 °C.

shows the Pd $3d_{5/2}$ XPS spectra of the PdO thin film annealed at different temperatures. The two chemical states, metal Pd and PdO, were used for the XPS curve fitting. As shown in Figure 6a, the Pd $3d_{5/2}$ XPS signal of the metal Pd state becomes obvious at 110 °C and is overwhelming over that of the PdO state at 125 °C. The Pd metal state is in the form of nanocrystals according to the high-resolution TEM (HRTEM) image shown in Figure 6b. Combining the above-discussed characterization results, we believe that nanosized Pd islands are also produced on the PdO thin film under the CO-gas-sensing condition at temperatures higher than 110 °C. However, the amount of metal Pd formed on the PdO thin film must be much smaller than that produced in the CO/N₂ gas mixture because Pd reoxidation should be vigorous under the oxygen-rich catalytic condition. As a result, the geometric shape and size of Pd nanoislands are greatly modified by the reoxidation reaction, leading to a smaller size of the Pd nanoislands compared with the nanocrystals shown in the HRTEM image.

Besides the PdO reduction, Pd reoxidation is also a key reaction step for the oscillatory CO response. The temperature at which Pd oxidation takes place in air is crucial for the understanding of the oscillatory response of the PdO thin film at 150 °C. To study the temperature range in which Pd oxidation occurs, we prepared a Pd thin film on the SiO₂ substrate by sputter deposition, and thermally annealed the thin film at different temperatures in the dry air for 20 min. Figure 7

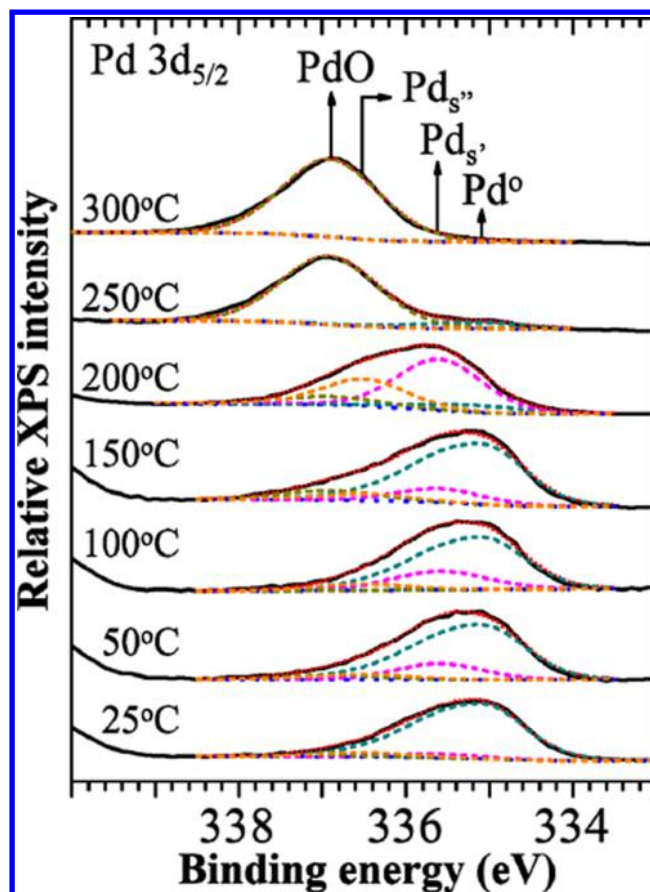


Figure 7. Pd $3d_{5/2}$ XPS spectra of Pd thin films thermally annealed in the dry air at different temperatures. The arrows indicate the binding energies corresponding to the surface chemical states of the thermally annealed PdO thin film. The labels, Pd_{s'} and Pd_{s''}, represent two different Pd surface sites that adsorb oxygen molecules.

presents Pd $3d_{5/2}$ XPS spectra of the Pd thin film as a function of the annealing temperature. Four-component peaks are necessary for the best curve fitting. The peak at 335.1 eV corresponds to metal Pd and the peak at 336.9 eV is due to the PdO state. The two peaks at 335.6 and 336.5 eV are associated with surface Pd atoms that adsorb oxygen.^{39,40} The Pd $3d_{5/2}$ peak due to the PdO component first becomes obvious when the sample is annealed at 150 °C, indicating that Pd oxidation reaction must begin in the temperature range between 100 and 150 °C. Because both the PdO reduction and the Pd oxidation reactions occur in the temperature range between 100 and 150 °C, the oscillatory sensing response of the PdO thin film at 150 °C can be related to the reactivity switching between the PdO reduction by the CO gas mixture and the reoxidation of the metal Pd, which is formed as a result of the PdO reduction.

In addition to the oscillatory response, the PdO thin film exhibits other CO-sensing behaviors at 150 °C dramatically different from that at lower temperatures. The conductance of the PdO thin film slightly drops right after the CO introduction and then rapidly increases before entering the oscillatory response regime. Because the two opposite changes in the conductance are both due to the introduction of the CO gas mixture, there must be two different reaction mechanisms in which CO molecules modify the surface of the PdO thin film. It is very likely that CO oxidation with anionic oxygen adspecies and CO-induced PdO reduction take place sequentially at 150

°C; the former causes the slight drop in the conductance, and the latter results in the rapid increase. The PdO reduction reaction is preceded by the CO oxidation reaction because oxygen adspecies must be depleted before CO molecules can directly interact with the PdO surface lattice. Metal Pd phases formed as a result of the PdO reduction by CO have the ability to dissociatively adsorb oxygen molecules from the gas mixture. For example, two types of oxygen adatoms have been identified to be present on the Pd(110) and -(111) surfaces at temperatures higher than 100 °C; they are the surface atomic state and the subsurface atomic state.^{41,42} The metal Pd phases are likely present on the PdO nanoflake in the form of nanosized islands as suggested previously. Negative charges can transfer from Pd nanoislands to electrophilic oxygen adatoms on the islands and can thus modify the electronic structure of the nearby region of the underlying PdO substrate. Figure 8

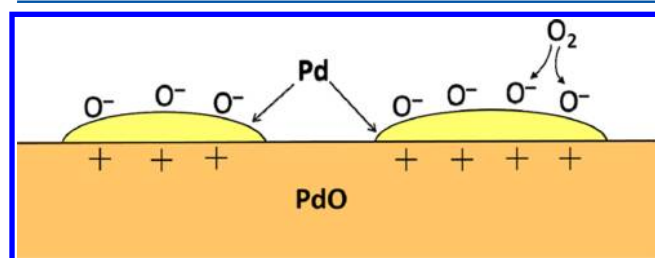


Figure 8. Schematic illustration of the removal of electrons from Pd nanoislands to oxygen adatoms resulting in the positive charge accumulation at the interface between Pd nanoislands and the PdO substrate. Oxygen molecules from the gas mixture are dissociatively adsorbed on the metal Pd islands.

schematically illustrates the charge transfer model, which describes how the dissociative adsorption of oxygen on Pd nanoislands increases the majority carrier concentration in the PdO thin film. The removal of electrons from Pd nanoislands leads to positive charge accumulation at the interface between Pd nanoislands and the PdO substrate, thus increasing the conductivity of the p-type PdO thin film. As described below, the charge transfer model can also be used to explain the observation of the conductance increase of the PdO thin film after the stop of the CO gas mixture flow.

When the CO gas is switched off, the recovery current at 150 °C quickly increases to a maximum before a deep drop. Without the CO gas, the PdO reduction reaction can no longer occur on the PdO thin film in the dry air. The immediate increase in the recovery current is likely to be related with the dissociative oxygen adsorption on residual Pd nanoislands, which have taken part in the oscillatory response reaction. At the initial stage of the oxidation reaction of residual Pd nanoislands in the dry air, dissociative oxygen adsorption on the Pd nanoislands will increase the conductivity of the PdO thin film via the above proposed charge transfer mechanism, which causes the conductivity rise before the oscillation regime. However, the coverage of metal Pd nanoislands and oxygen adatoms gradually diminishes with the oxidation time and finally reaches a critical value at which the density of positive charge accumulated at the interface between the PdO substrate and the Pd nanoislands begins to decrease, leading to the observation of the inverse change in the conductance of the PdO thin film. Note that the conductance and the sensing current drop of the PdO thin film becomes lower by each sensing cycle (see Figure 3). The successive decreases in the

conductivity must be due to an irreversible modification on the surface properties of the PdO thin film. Due to the surface modification, fewer surface sites are available for CO-activated reactions on the thin film after each sensing cycle, thus resulting in the decrease in the response sensitivity of the thin film toward CO. It is worth mentioning that, on the basis of the observation of delicate changes in the PdO conductance upon the CO exposure, we believe that the electrical measurement may be a useful method providing valuable clues to a better understanding of the reaction kinetics of the CO oxidation on Pd catalysts.

At temperatures higher than 150 °C, the sensing current of the PdO thin film drops exponentially upon the CO exposure. The quick drop of the conductance indicates that the CO sensing mechanism at 200 and 250 °C is distinctly different from that at 150 °C. The metal Pd phase must not be extensively formed on the PdO surface at the high temperatures, and therefore, the charge transfer mechanism that occurs at 150 °C is inactive at these temperatures. It is likely that CO adsorption on the PdO surface is kinetically unfavorable at the high temperatures, and therefore, the PdO reduction by CO via the Langmuir–Hinshelwood (L-H) mechanism is unimportant. The primary reaction channel for the PdO reduction thus follows the Eley–Rideal (E-R) mechanism, which may be active only for specific surface lattice orientations, such as the (100) plane.³³ As a result, the coverage of the metal Pd phase is too trivial to significantly affect the conductance of the PdO thin film via the charge transfer mechanism. The conductance drop upon the CO exposure at 200 and 250 °C may be explained as follows. It has been widely believed that peroxide ions (O_2^{2-}) are adsorbed on semiconductor oxides at temperatures above 150 °C,^{43,44} although the direct evidence of its presence is lacking.⁴⁵ If the peroxide ion is a stable adspecies on the PdO thin film, the CO oxidation by O_2^{2-} ions can induce a conductance drop via the similar ionosorption mechanism as the CO oxidation by O_2^- ions at low temperatures. Moreover, the reduction–reoxidation mechanism, which is described by the oxygen-vacancy model, is also a likely cause responsible for the change in the conductance of the PdO thin film at high temperatures.^{20,46} The PdO reduction by CO at high temperatures can proceed via the E-R kinetics, producing surface oxygen vacancies on the PdO thin film. The surface oxygen vacancies can further diffuse into the thin film, thereby increasing the density of free electrons in the thin film and thus decreasing the conductivity of the p-type oxide. On the other hand, after the switch-off of the CO gas flow, reoxidation of the PdO thin film in the dry air reduces the density of oxygen vacancies, thereby restoring the conductivity of the thin film.

Pd is often doped in SnO_2 to improve the gas-sensing response and selectivity of the n-type oxide toward reducing gases, such as H_2 and CO.^{47–49} It is worthwhile to examine if any similarity exists between Pd-doped SnO_2 sensors and the PdO thin film in the enhancement effect of Pd on the gas-sensing response. However, most reported Pd-doped SnO_2 sensors have a much smaller Pd content than the PdO thin film and were operated at a higher sensing temperature. Moreover, the gas-sensing response of Pd-doped SnO_2 sensors greatly depends on the Pd loading method⁴⁹ and the dispersion state of Pd additives, such as particle size and uniformity.⁵⁰ In a study on the Pd-doped SnO_2 gas sensor by operando X-ray absorption spectroscopy, Koziej et al. observed that the sensor doped with 0.2 wt % Pd showed little change in the oxidation

state of Pd when exposed to 50 ppm CO in dry air at 300 °C but had a high sensor signal.⁵¹ On the other hand, the 3 wt % Pd sensor had a slight change toward more reduced Pd particles in the presence of CO/air at 300 °C. They concluded that Pd was dispersed at an atomic level or as very small clusters at the low Pd content under real CO sensing conditions and suggested that the local/surface Pd site effect on the enhanced CO sensing response was much more important than the two conventional models used to explain the role of Pd additives in gas sensing, i.e., the electronic effect mechanism and the spillover mechanism. Because the Pd atomic content of the PdO thin film is as large as 50%, the Pd effect on the CO sensing kinetics of the PdO sensor is likely different from SnO₂ sensors slightly doped with Pd. As discussed above, metal Pd must be formed on the PdO thin film at 150 °C in the CO/dry air gas mixture, as revealed by the oscillatory response and the abnormal conductance increase, which is ascribed to the formation of nanosized Pd particles. However, at the present time, we are unable to provide operando evidence of the formation of Pd nanoparticles at 150 °C under the CO-gas-sensing condition, although the ex-situ TEM analysis showed that Pd nanoparticles were formed on the PdO thin film below 150 °C in the reducing CO/N₂ gas mixture. To investigate if Pd nanoparticles are formed in the CO/dry air gas mixture at 150 °C, we are undertaking rapid quench experiments for the PdO sensor using a fast N₂ flow instead of the dry air. We expect that the rapid quench treatment may prevent nanosized Pd domains from quick reoxidation after the gas-sensing measurement and allows us to study these Pd domains by TEM and XPS.

Figure 9 shows the CO sensor signal of the PdO thin film as a function of the sensing temperature for different CO

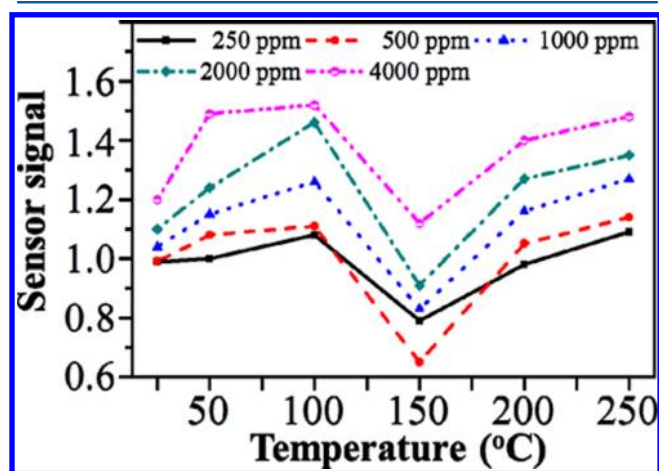


Figure 9. The plot of the sensor signal as a function of the sensing temperature for different CO concentrations.

concentrations. The sensor signal (R/R_0) is herein defined for the p-type PdO semiconductor by the ratio of the resistance of the PdO thin film under the CO exposure (R) to that in the dry air (R_0). From the sensor signal–temperature (S – T) curves, the PdO thin film has a sensor signal increasing with the CO concentration, and the sensor exhibits the best CO sensing response at 100 °C. Most interestingly, the S – T curves show a large dip at 150 °C for all the CO concentrations under test. The observation of the dip is certainly related to the complex surface kinetics on the PdO thin film at 150 °C, at which the conductance of the oxide increases before the oscillatory

sensing behavior occurs. The PdO thin film exhibits a sensor signal smaller than 1 at 150 °C except for the CO exposure at 4000 ppm. The sensor signal is even as low as 0.65 for the CO exposure at 500 ppm. The large inverse change in the sensor signal is rarely reported in the literature and may provide a potential application for CO sensors of high selectivity. In order to investigate the selectivity of the PdO sensor, we have also studied the sensing response of the PdO thin film toward H₂, CH₄, and CO₂ gases. Exposure of these gases at temperatures below 250 °C results in a decrease in the conductance of the PdO thin film as well. Compared with the CO gas mixture, the PdO sensor has a higher sensing sensitivity toward H₂, with a lower sensitivity toward CH₄ and CO₂. For instance, the PdO thin film shows a sensor signal of 1.28 and 1.88 upon the exposure of 250 ppm of H₂ at 50 and 100 °C, respectively. However, H₂ does not show the oscillatory sensing response at 150 °C, and PdO always exhibits a sensor signal larger than 1 for H₂ at temperatures below 250 °C. On the basis of the inverse change in the sensor signal of the PdO thin film toward CO at 150 °C, we can design a CO gas sensor of high selectivity. When two PdO sensing elements, which operate independently at 150 °C and at a lower temperature, e.g., 50 °C, are integrated into a sensor system with separate sensing readouts, the two elements can produce opposite electrical responses to the gas mixture with a CO concentration as low as 500 ppm. One can thus distinguish the sensing response due to the CO exposure from that due to the exposure of other gases, such as H₂ and CH₄, to which PdO always has a sensor signal larger than 1.

4. CONCLUSIONS

PdO nanoflake thin films were prepared by reactive sputter deposition for the study of CO gas sensing at temperatures below 250 °C. The flakelike PdO nanostructures provide a large open surface area allowing for rapid and extensive CO adsorption on the thin film. The PdO thin film exhibits a complicated CO sensing behavior within the studied temperature range. At temperatures at 100 °C and below, the electrical conductance of the thin film drops upon the exposure of the CO/dry air gas mixture. The CO sensing behavior can be described simply by the oxygen ionosorption model. At 150 °C, the PdO thin film shows a rapid increase in the conductance upon the CO exposure before entering the oscillatory response regime. The oscillatory response occurs only when the CO concentration is larger than 1500 ppm and is due to the reactivity switching between the PdO reduction and reoxidation reactions. The conductance increase before and after the oscillatory response is ascribed to the positive charge accumulation at the interface between the PdO substrate and metal Pd nanoislands, which are formed in the PdO reduction reaction. The charge accumulation is a result of the charge transfer between the Pd nanoislands and oxygen adatoms on them. At temperatures higher than 150 °C, the conductance drops when the PdO thin film is exposed to CO. In addition to the ionosorption model, the oxygen vacancy model can be used to account for the CO sensing response of the PdO thin film in the high-temperature regime. On the basis of the observation that the PdO thin film has an opposite change in the sensing sensitivity at 150 °C, a CO sensor system of high selectivity, which integrates two PdO sensing elements operating independently at 150 °C and a lower temperature, is proposed. Because the gas-sensing test demonstrated delicate changes in the PdO conductance upon the CO exposure, we think that the electrical measurement method may provide valuable informa-

tion about the reaction kinetics of the CO oxidation on Pd catalysts under a fuel-lean condition.

AUTHOR INFORMATION

Corresponding Author

*E-mail: fmpan@faculty.nctu.edu.tw. Tel: 886-3-5131322. Fax: 886-3-5724727.

Notes

The authors declare no competing financial interest.

ACKNOWLEDGMENTS

The financial support of the National Science Council of the Republic of China (NSC99-2221-E-009-109-MY3) is gratefully acknowledged.

REFERENCES

- (1) Zhuiykov, S. Carbon Monoxide Detection at Low Temperatures by Semiconductor Sensor with Nanostructured Au-Doped CoOOH Films. *Sens. Actuators, B* **2008**, *129*, 431–441.
- (2) Stetter, J. R.; Lin, J. Amperometric Gas Sensors—A Review. *Chem. Rev.* **2008**, *108*, 352–366.
- (3) Gaspera, E. D.; Buso, D.; Guglielmi, M.; Martucci, A.; Bello, V.; Mattei, G.; Post, M. L.; Cantalini, C.; Agnoli, S.; Granozzi, G.; Sadek, A. Z.; Kourosh, K. Z.; Wlodarski, W. Comparison Study of Conductometric, Optical and SAW Gas Sensors Based on Porous Sol–Gel Silica Films Doped with NiO and Au Nanocrystals. *Sens. Actuators, B* **2010**, *143*, 567–573.
- (4) Mattei, G.; Mazzoldi, P.; Post, M. L.; Buso, D.; Guglielmi, M.; Martucci, A. Cookie-like Au/NiO Nanoparticles with Optical Gas-Sensing Properties. *Adv. Mater.* **2007**, *19*, 561–564.
- (5) Martucci, A.; Bassiri, N.; Guglielmi, M.; Armelao, L.; Gross, S.; Pivin, J. C. NiO–SiO₂ Sol–Gel Nanocomposite Films for Optical Gas Sensor. *J. Sol–Gel Sci. Technol.* **2003**, *26*, 993–996.
- (6) Park, J. A.; Moon, J. H.; Lee, S. J.; Kim, S. H.; Zyung, T. H.; Chu, H. Y. Structure and CO Gas Sensing Properties of Electrospun TiO₂ Nanofibers. *Mater. Lett.* **2010**, *64*, 255–257.
- (7) Akbar, S. A.; Younkman, L. B. Sensing Mechanism of a Carbon Monoxide Sensor Based on Anatase Titania. *J. Electrochem. Soc.* **1997**, *144*, 1750–1753.
- (8) Wang, J. X.; Sun, X. W.; Yang, Y.; Huang, H.; Lee, Y. C.; Tan, O. K.; Vayssieres, L. Hydrothermally Grown Oriented ZnO Nanorod Arrays for Gas Sensing Applications. *Nanotechnology* **2006**, *17*, 4995–4998.
- (9) Chang, S. J.; Hsueh, T. J.; Chen, I. C.; Huang, B. R. Highly Sensitive ZnO Nanowire CO Sensors with the Adsorption of Au Nanoparticles. *Nanotechnology* **2008**, *19*, 175502.
- (10) Wei, S. H.; Yu, Y.; Zhou, M. H. CO Gas Sensing of Pd-doped ZnO Nanofibers Synthesized by Electrospinning Method. *Mater. Lett.* **2010**, *64*, 2284–2286.
- (11) Hung, N. L.; Kim, H. J.; Hong, S. K.; Kim, D. J. Enhancement of CO Gas Sensing Properties in ZnO Thin Films Deposited on Self-Assembled Au Nanodots. *Sens. Actuators, B* **2010**, *151*, 127–132.
- (12) Kolmakov, A.; Zhang, Y. X.; Cheng, G. S.; Moskovits, M. Detection of CO and O₂ Using Tin Oxide Nanowire Sensors. *Adv. Mater.* **2003**, *15*, 997–1000.
- (13) Zhang, T.; Liu, L.; Qi, Q.; Li, S. C.; Lu, G. Y. Development of Microstructure In/Pd-doped SnO₂ Sensor for Low-Level CO Detection. *Sens. Actuators, B* **2009**, *139*, 287–291.
- (14) Bahrami, B.; Khodadadi, A.; Kazemeini, M.; Mortazavi, Y. Enhanced CO Sensitivity and Selectivity of Gold Nanoparticles-Doped SnO₂ Sensor in Presence of Propane and Methane. *Sens. Actuators, B* **2008**, *133*, 352–356.
- (15) Huang, H.; Ong, C. Y.; Guo, J.; White, T.; Tse, M. S.; Tan, O. K. Pt Surface Modification of SnO₂ Nanorod Arrays for CO and H₂ Sensors. *Nanoscale* **2010**, *2*, 1203–1207.
- (16) Liao, L.; Zhang, Z.; Yan, B.; Zheng, Z.; Bao, Q. L.; Wu, T.; Li, C. M.; Shen, Z. X.; Zhang, J. X.; Gong, H.; Li, J. C.; Yu, T.

Multifunctional CuO Nanowire Devices: *p*-Type Field Effect Transistors and CO Gas Sensors. *Nanotechnology* **2009**, *20*, 085203.

(17) Patil, D.; Patil, P.; Subramanian, V.; Joy, P. A.; Potdar, H. S. Highly Sensitive and Fast Responding CO Sensor Based on Co₃O₄ Nanorods. *Talanta* **2010**, *81*, 37–43.

(18) Cao, A. M.; Hu, J. S.; Liang, H. P.; Song, W. G.; Wan, L. J.; He, X. L.; Gao, X. G.; Xia, S. H. Hierarchically Structured Cobalt Oxide (Co₃O₄): The Morphology Control and Its Potential in Sensors. *J. Phys. Chem. B* **2006**, *110*, 15858–15863.

(19) Korotcenkov, G. Metal Oxides for Solid-State Gas Sensors: What Determines Our Choice? *Mater. Sci. Eng., B* **2007**, *139*, 1–23.

(20) Gurlo, A.; Riedel, R. In Situ and Operando Spectroscopy for Assessing Mechanisms of Gas Sensing. *Angew. Chem., Int. Ed.* **2007**, *46*, 3826–3848.

(21) Zemel, J. N. Theoretical Description of Gas–Film Interaction on SnOx. *Thin Solid Films* **1988**, *163*, 189–202.

(22) Franke, M. E.; Koplone, T. J.; Simon, U. Metal and Metal Oxide Nanoparticles in Chemiresistors: Does the Nanoscale Matter? *Small* **2006**, *2*, 36–50.

(23) Wang, C. X.; Yin, L. W.; Zhang, L. Y.; Xiang, D.; Gao, R. Metal Oxide Gas Sensors: Sensitivity and Influencing Factors. *Sensors* **2010**, *10*, 2088–2106.

(24) Li, W. C.; Shen, C. S.; Wu, G. G.; Ma, Y.; Gao, Z. M.; Xia, X. C.; Du, G. T. New Model for a Pd-Doped SnO₂-Based CO Gas Sensor and Catalyst Studied by Online in-Situ X-ray Photoelectron Spectroscopy. *J. Phys. Chem. C* **2011**, *115*, 21258–21263.

(25) Hubner, M.; Simion, C. E.; Haensch, A.; Barsan, N.; Weimar, U. CO Sensing Mechanism with WO₃ Based Gas Sensors. *Sens. Actuators B* **2010**, *151*, 103–106.

(26) Kohl, D. Function and Applications of Gas Sensors. *J. Phys. D: Appl. Phys.* **2001**, *34*, R125–R149.

(27) Fierro, J. L. G.; Garcia de la Branda, J. F. Chemisorption of Probe Molecules on Metal Oxides. *Catal. Rev.: Sci. Eng.* **1986**, *28*, 265–333.

(28) Le Page, J. F. *Applied Heterogeneous Catalysis: Design, Manufacture, Use of Solid Catalysts*, Edition Technip: Paris, 1978.

(29) Huang, C. J.; Pan, F. M.; Chen, H. Y.; Chang, L. Growth and Photoresponse Study of PdO Nanoflakes Reactive-Sputter Deposited on SiO₂. *J. Appl. Phys.* **2010**, *108*, 053105.

(30) Hinojosa, J. A., Jr.; Kan, H. H.; Weaver, J. F. Molecular Chemisorption of O₂ on a PdO(101) Thin Film on Pd(111). *J. Phys. Chem. C* **2008**, *112*, 8324–8331.

(31) Specchia, S.; Finocchio, E.; Busca, G.; Palmisano, P.; Specchia, V. Surface Chemistry and Reactivity of Ceria–Zirconia-Supported Palladium Oxide Catalysts for Natural Gas Combustion. *J. Catal.* **2009**, *263*, 134–145.

(32) Forzatti, P. Status and Perspectives of Catalytic Combustion for Gas Turbines. *Catal. Today* **2003**, *83*, 3–18.

(33) Hirvi, J. T.; Kinnunen, T.-J. J.; Suvanto, M.; Pakkanen, T. A.; Nørskov, J. K. CO Oxidation on PdO Surfaces. *J. Chem. Phys.* **2010**, *133*, 084704.

(34) Royer, S.; Duprez, D. Catalytic Oxidation of Carbon Monoxide over Transition Metal Oxides. *ChemCatChem* **2011**, *3*, 24–65.

(35) Eiswirth, M.; Möller, P.; Wetzl, K.; Imbihl, R.; Ertl, G. Mechanisms of Spatial Selforganization in Isothermal Kinetic Oscillations during the Catalytic CO Oxidation on Pt Single Crystal Surfaces. *J. Chem. Phys.* **1989**, *90*, 510.

(36) Ehsasi, M.; Berdau, M.; Rebitzki, T.; Charlé, K. P.; Christmann, K.; Block, J. H. A Reactive Phase Diagram of CO Oxidation on Pd(110): Steady and Oscillatory States. *J. Chem. Phys.* **1993**, *98*, 9177.

(37) Bondzie, V. A.; Kleban, P. H.; Dwyer, D. J. Kinetics of PdO Formation and CO Reduction on Pd(110). *Surf. Sci.* **2000**, *465*, 266–276.

(38) Hendriksen, B. L. M.; Bobaru, S. C.; Frenken, J. W. M. Oscillatory CO Oxidation on Pd(100) Studied with In Situ Scanning Tunneling Microscopy. *Surf. Sci.* **2004**, *552*, 229–242.

(39) Lundgren, E.; Kresse, G.; Klein, C.; Borg, M.; Andersen, J. N.; De Santis, M.; Gauthier, Y.; Konvicka, C.; Schmid, M.; Varga, P. Two-Dimensional Oxide on Pd(111). *Phys. Rev. Lett.* **2002**, *88*, 246103.

(40) Zemlyanov, D.; Aszalos-Kiss, B.; Kleimenov, E.; Teschner, D.; Zafeiratos, S.; Hävecker, M.; Knop-Gericke, A.; Schlögl, R.; Gabasch, H.; Unterberger, W.; Hayek, K.; Klötzer, B. In Situ XPS Study of Pd(111) Oxidation. Part 1: 2D Oxide Formation in 10^{-3} mbar O_2 . *Surf. Sci.* **2006**, *600*, 983–994.

(41) Gorodetskii, V. V.; Matveev, A. V.; Kalinkin, A. V.; Nieuwenhuys, B. E. Mechanism for CO Oxidation and Oscillatory Reactions on Pd Tip and Pd(110) Surface: FEM, TPR, XPS Studies. *Chem. Sust. Develop.* **2003**, *11*, 67–74.

(42) Gorodetskii, V. V.; Matveev, A. V.; Podgornov, E. A.; Zaera, F. Study of the Low-temperature Reaction between CO and O_2 over Pd and Pt Surfaces. *Top. Catal.* **2005**, *32*, 17–28.

(43) Chang, S. C. Oxygen Chemisorption on Tin oxide: Correlation between Electrical Conductivity and EPR Measurements. *J. Vac. Sci. Technol.* **1980**, *17*, 366–369.

(44) Kocemba, I.; Rynkowski, J. M. The Effect of Oxygen Adsorption on Catalytic Activity of SnO_2 in CO Oxidation. *Catal. Today* **2011**, *169*, 192–199.

(45) Gurlo, A. Interplay between O_2 and SnO_2 : Oxygen Ionosorption and Spectroscopic Evidence for Adsorbed Oxygen. *ChemPhysChem* **2006**, *7*, 2041–2052.

(46) Tricoli, A.; Righettoni, M.; Teleki, A. Semiconductor Gas Sensors: Dry Synthesis and Application. *Angew. Chem., Int. Ed.* **2010**, *49*, 7632–7659.

(47) Safonova, O. V.; Delabouglise, G.; Chenevier, B.; Gaskov, A. M.; Labeau, M. CO and NO_2 Gas Sensitivity of Nanocrystalline Tin Dioxide Thin Films Doped with Pd, Ru and Rh. *Mater. Sci. Eng. C-Mater. Biol. Appl.* **2002**, *21*, 105–111.

(48) Barsan, N.; Koziej, D.; Weimar, U. Metal Oxide-Based Gas Sensor Research: How To? *Sens. Actuators, B* **2007**, *121*, 18–35.

(49) Koziej, D.; Barsan, N.; Shimanoe, K.; Yamazoe, N.; Szuber, J.; Weimar, U. Spectroscopic Insights into CO Sensing of Undoped and Palladium Doped Tin Dioxide Sensors Derived from Hydrothermally Treated Tin Oxide Sol. *Sens. Actuators, B* **2006**, *118*, 98–104.

(50) Yuasa, M.; Masaki, T.; Kida, T.; Shimanoe, K.; Yamazoe, N. Nano-sized PdO Loaded SnO_2 Nanoparticles by Reverse Micelle Method for Highly Sensitive CO Gas Sensor. *Sens. Actuators, B* **2009**, *136*, 99–104.

(51) Koziej, D.; Hübner, M.; Barsan, N.; Weimar, U.; Sikora, M.; Grunwaldt, J.-D. Operando X-ray Absorption Spectroscopy Studies on Pd- SnO_2 Based Sensors. *Phys. Chem. Chem. Phys.* **2009**, *11*, 8620–8625.